

DESIGN AND PERFORMANCE ANALYSIS OF 28 GHZ MIMO ANTENNA FOR 5G COMMUNICATIONS

Irfan Ali¹, Malik Shehram Khan², Bilal Ur Rehman^{*3}, Kifayat Ullah⁴, Humayun Shahid⁵, Jin Zhu⁶

^{1,6}Ocean College, Jiangsu University of Science and Technology, China

^{2, *3,4}Department of Electrical Engineering, University of Engineering and Technology, Peshawar

⁵Department of Telecommunication Engineering, University of Engineering and Technology, Taxila

DOI: <https://doi.org/10.5281/zenodo.15797246>

Keywords

5G, Microstrip Patch Antenna, MIMO Antenna

Article History

Received on: 28 May, 2025

Accepted on: 28 June, 2025

Published on: 03 July, 2025

Copyright @Author

Corresponding Author: *

Bilal Ur Rehman

Abstract

This research examines the specifications of the 5G mobile communication network. The arrangement distinctly illustrates the two conventional semi-circular microstrip patches of the MIMO antennas operating at 28 GHz. The antenna employs embedded feeding technology, with Rogers RT/duroid 5880 as the dielectric substrate. The antenna dimensions are 18mm x 36mm x 0.8mm. The Defected Ground Structure (DGS) is groove-deflected on the ground plane to enhance impedance bandwidth and optimize isolation performance; therefore, the impedance-matching bandwidth is 5.6 GHz, substantially augmenting the antenna's frequency flexibility. Furthermore, the design incorporates a T-shaped slot in the chosen optimization, mitigating electromagnetic interference among the antenna parts. The test findings indicate that the antenna will exhibit a reflection coefficient (S11) below -10 dB within the frequency range of 24.9 GHz to 30.5 GHz, and the mutual coupling (S21) will be below -40 dB. The Envelope Correlation Coefficient (ECC) is below 0.005, the radiation efficiency is above 95, and the diversity gain (DG) surpasses 9.99 dB, therefore fully satisfying the performance criteria for 5G communication systems. The MIMO arrangement minimizes return loss and broadens operational bandwidth. Consequently, it results in tasks characterized by minimum mutual coupling, thereby substantially improving the major performance parameters of directivity, gain, and radiation efficiency.

INTRODUCTION

The 5G technology represents a significant transformation in wireless communications due to its exceptionally high data speeds, minimal latency, and enhanced dependability [1]. The deficiencies of legacy systems encompass the necessity to incorporate Multiple Input Multiple Output (MIMO) antennas, which have emerged as a crucial research focus in 5G networks. Not only does MIMO technology reduce the complexity of single-antenna systems, but it also facilitates higher-order

functionalities like a massive MIMO, beamforming, and multi-user MIMO (MU-MIMO) and completely transforms the performance and the ability of the contemporary wireless communication system infrastructure [2]. MIMO antennas have much potential for secure communications with flexible applications in departments such as commercial, industrial, and satellite communications, green radio technologies, military systems, ZigBee networks, and wireless body area networks (WBANs) [3].

2. LITERATURE REVIEW

MIMO antennas are an essential component of 5G communication networks, creating a basis for the structural design and optimization of next-generation wireless networks. The MIMO antennas provide high signal quality compared to the traditional single-antenna systems and can cover sub-6 GHz and mm-wave frequency bands in 5G networks [4]. The preference for the mm-wave frequencies comes with an exclusive challenge: high signal attenuation properties and susceptibility to physical barriers [5]. To overcome these problems, MIMO antennas are used with advanced signal processing, such as beamforming, which can boost the signal and transmission stability. The right Channel propagation models are also crucial in creating new mm-wave signaling protocols since it is through this that spatial domain variability in MIMO systems can be highly characterized and still achieve excellent spectral efficiency [6]. The diversity offered by MIMO antenna systems is achieved by the spatial orthogonal Conditions of Channel responses, and this delivers universal performance to these Antenna systems in each wide range of propagation conditions. Microstrip antenna solutions tend to be favored more in the applications of MIMO, like their low cost, ease of construction and manufacturing, and straightforwardness in their design in a way that the transistors are conveniently integrated with the miniaturized and high-performance wireless systems [7]. Although MIMO design and implementation impose many problems, they eventually improve antenna performance [8]. Key design criteria include sufficient isolation and robust mutual interaction with adjacent antenna elements to provide compact MIMO configurations. The antenna parts of MIMO systems often require broad lobe patterns, substantial gain, and sufficient separation to provide a minimal bit error rate (BER) and to optimize Channel capacity [9]. The properties are crucial for leveraging spatial diversity and reducing the impacts of multipath fading, particularly in higher frequency bands where signal attenuation and absorption are more pronounced [10]. High-gain antennas are often required to counteract such attenuations, and a more cost-effective and straightforward planar MIMO configuration is favored. The recent rapid advancements in wireless communication facilitated

the implementation of the Massive MIMO (M-MIMO) technology, which was introduced during the 5G standardization process. Scientists are anticipating the advancement of new technology to optimize its use as it emerges as a fundamental component of future communication networks.

In future 5G networks, Massive MIMO (M-MIMO) will be pivotal in enhancing communication system Channel capacity and optimizing spectral efficiency [11]. This technology operates across diverse frequency bands to meet the multifaceted demands of next-generation wireless networks [12]. Notably, several leading Chinese institutions are actively advancing MIMO antenna research. For example, Xi'an University of Technology is engaged in cutting-edge studies on MIMO antenna design, while Qingdao University of Science & Technology and Nanjing University of Aeronautics and Astronautics are focusing on MIMO applications for 5G communications, with particular emphasis on reducing mutual coupling between antenna elements [13]. Chongqing University of Posts and Telecommunications has researched millimetre-wave MIMO technologies, with its team designing a four-port MIMO antenna that employs slotted patches to enhance isolation and gain. Researchers at Nanjing University of Aeronautics and Astronautics has developed a MIMO antenna for 5G dual mm-wave bands (N257/N258 and N262), utilizing slotted ground structures to diminish mutual coupling and enhance impedance matching. Nanjing University of Information Science and Technology has made notable advancements in MIMO antenna design and optimization [14]-[18]. Further, the low mutual coupling performance of the MIMO antenna is discussed in [19, 20].

An Antenna transmits or receives radio waves [21]. Antennas are pivotal components in wireless communication systems. They work as transducers, converting the guided electrical signals into electromagnetic waves and vice versa [22]. This ability to transmit and receive electromagnetic signals makes them integral to various applications, including radio, television, radar, mobile communications, and satellite systems. MIMO systems rely on Channel estimation to understand how signals have traversed the wireless medium. It involves determining the effects of the Channel,

such as fading, phase shifts, and interference on each signal. Training sequences, often called pilot signals, are transmitted alongside the data to assist the receiver in determining the Channel's characteristics, enabling the correct separation of data streams. Channel estimation is crucial for effectively demultiplexing spatially multiplexed signals [23]. MIMO has an advantage over SISO in the sense that it has the potential to deliver more than one signal at any point in time. Hence, the existing capacity can serve the same purpose of providing more data without requiring additional bandwidth [24]. An increase in data rates results in improved user performance, especially for applications and services requiring high bandwidth, such as videos, video games, and larger files. Today's mobile networks benefit from MIMO by enhancing users' smooth and fast functionality. Spectral efficiency can be defined as the data rate per unit bandwidth, and its unit of measurement is bps/Hz. However, MIMO systems can provide throughputs higher than SISO systems using two data streams on the two paths sent simultaneously. This results in a good utilization of the available spectrum and, hence, a good service provision [25]. Since MIMO transmits more data in a bandwidth, it lowers the latency and increases the transmission rate [26].

On the other hand, MIMO can take advantage of different antennas and, therefore, increase the probability of avoiding multipath fading [27]. The diversity gain characteristic of MIMO systems implies a low BER. As a result, MIMO systems can be used to achieve a reliable communication link with high interference or a rapidly varying environment [28]. Using multiple antennas, MIMO systems increase coverage by improving the quality of signals and or reducing the areas of no signal reception. This most straightforward form of MIMO antennas involves using other complex techniques that only direct signals at the intended users without transmitting in all directions. It will also entail the presence of a more potent and reliable signal to all the users located from the transmitter centre [29]. The above results show that a high degree of energy directivity towards the receiver enhances the coverage of MIMO systems. Users in weak signal places, including indoor zones or on the peripheries of the signal coverage zone, enjoy improved signal quality and

stability [30]. MIMO antennas are essential in military and defence applications, providing secure and reliable communication. MIMO technology enhances the security of communication systems in defence operations, protecting sensitive information from interception. Encrypted communications can be maintained even in hostile environments [31].

A recent study introduced two semi-circular microstrip patch MIMO antennas operating at 28 GHz, tailored for 5G mobile applications. The antennas utilize Rogers RT/duroid 5880 as a substrate and incorporate an embedded feeding mechanism within a compact 18mm × 36mm × 0.8mm footprint. The design integrates a groove-shaped Defected Ground Structure (DGS) and a T-shaped slot to enhance impedance bandwidth and reduce mutual coupling. These modifications result in an impressive bandwidth of 5.6 GHz, return loss below -10 dB from 24.9 to 30.5 GHz, and mutual coupling (S21) lower than -40 dB. Additionally, the antennas exhibit high radiation efficiency (over 95%), low Envelope Correlation Coefficient (ECC < 0.005), and excellent diversity gain (>9.99 dB). Such characteristics confirm the antenna's strong suitability for integration into modern 5G devices, where high isolation and wideband performance are critical.

3. DESIGN AND SIMULATION OF SINGLE ELEMENT ANTENNA

A semicircular patch antenna has been constructed for 5G applications. A circular patch antenna is first constructed utilizing the Rogers RT/droid 5880 substrates, and its radius R is determined for operation at 28 GHz employing the subsequent equation.

$$R = \frac{F}{2\pi f\sqrt{\epsilon_r}} \quad (1)$$

Where $F = 8.7 \times 10^9$, f signifies the operational frequency (28 GHz in this instance), and ϵ_r indicates the relative permittivity of the substrate (Rogers).

The antenna designer alters the circular patch radiator into a semicircular configuration to meet the requirements of the 5G antenna. The semicircular patch necessitates a 50-ohm feed line for power transmission, which dictates its dimensions via formulae.

$$Z_0 = \frac{60}{\sqrt{\epsilon_r}} \ln\left(\frac{8h}{w} + \frac{w}{4h}\right) \quad (2)$$

Where Z_0 is the characteristic impedance (50 ohms), h represents the substrate's height, w represents the width of the microstrip line

The design establishes radio frequency coverage between 25 GHz to 30 GHz. The achievement of this requires etching a rectangular slot within the radiator structure. The slot dimensions can be calculated through:

$$f_s = \frac{c}{2L\sqrt{\epsilon_r}} \quad (3)$$

Where f_s is the slot resonance frequency, L is the length of the slot, c is the speed of light.

The calculation of inset length and width for inset feeding requires the below formula to achieve 50-ohm feed line impedance matching:

The antenna's performance relies heavily on its complete length, L , and width dimension W , as shown in Figure 1. Implementing the semicircular patch antenna demands adherence to multiple important procedures and essential design points. A circular patch design is the base framework to generate straight calculations for dimension

requirements based on frequency parameters. After reshaping the design from circular to semicircular, the antenna size was reduced without compromising the required resonance properties. The design works well under 5G frequency conditions because it fits into confined areas.

To achieve optimal power transfer, selecting a 50-ohm feed line for impedance matching between the antenna and transmission line is crucial. The dimensions of the feed line need to match the substrate characteristics, which shows the need for precise material evaluation during antenna planning. The rectangular radiator slot enables the adjustment of various parameters to obtain the needed frequency band. Modifying patch antenna geometry enables performance adjustment through significant effects on antenna parameters. Further, the inset feed technique improves the antenna's performance. It is a straightforward method of improving impedance matching—the proposed design approach's ability to work within the pre-allocated frequency band.

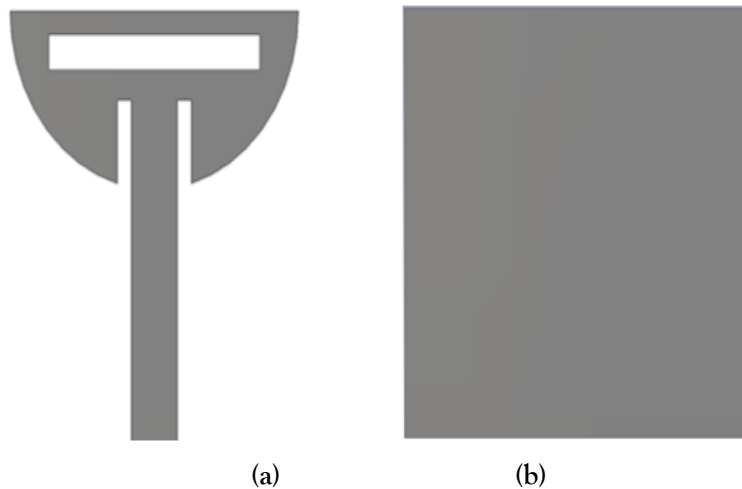


Figure 1: (a) Front View of Single Element Antenna, (b) Bottom View of Single Element Antenna

In the 25–30 GHz frequency range, the semicircular patch antenna's typical return loss is indicated by the simulated S_{11} value in Figure 2. According to radiation testing, the effective operating frequency band is -10 dB, and the terminal antenna guarantees S_{11} values in this range. In particular, it exhibits the lowest S_{11} value in the core 5G frequency band, which is around 28 GHz. That is why the proposed antenna provides very satisfactory results for the entire range of the given frequency band. At the

same time, the S_{11} is also an essential factor when it comes to the wideband designs needed for the 5G systems. A broad and massive operation enables the antenna to cater to a variety of multi-channel 5G services, along with serving the needs of the modern communication system. Depending on this, the S_{11} results suggest that the antenna provides the best design and thus can be used for 5G networks connected to it due to its high performance.

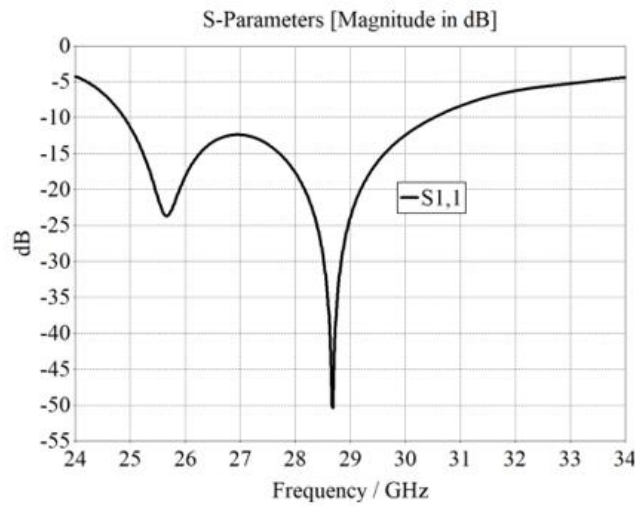


Figure 2: S-Parameter S11 of Single Antenna Element

Radiation Characteristics of Single Element Antenna

The radiation pattern supplied by the Antenna presents a graphical representation of how radiated power is distributed across space in-terms of direction. It demonstrates an antenna's capability to receive or transmit signals in various directions. The radiation pattern is usually examined on two principal planes: the E-plane (electric field plane) and the H-plane (magnetic field plane). The patterns are used to determine the directivity and coverage range of the Antenna.

Figure 3(a) Radiation Pattern at 26 GHz suggests that the main lobe of the electric field plane and magnetic field planes' main lobe is relatively broad. The wide main lobe indicates that the Antenna broadly covers the energy radiated in many directions, which makes it good at omnidirectional coverage. The wide pattern is helpful when it is necessary to send or receive signals in all directions and maintain a stable signal at different locations within the Antenna.

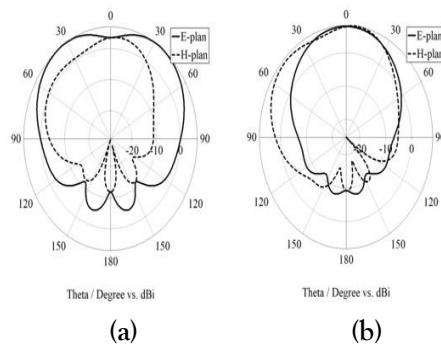


Figure 3: (a) Radiation Pattern at 26 GHz, (b) Radiation Pattern at 28 GHz

The radiation pattern at 28 GHz, depicted in Figure 3(b), shows a more focused main lobe compared to the pattern at 26 GHz. Hence, it indicates an increase in directivity, meaning that more radiated energy is concentrated in a specific direction. A more focused pattern is advantageous for 5G applications that require targeted communication, as it boosts the

signal strength and quality in the desired direction while attenuating interference from other directions. This increased directivity helps maintain strong and reliable connections in high-density urban environments. The radiation pattern at 29 GHz, also shown in Figure 4, exhibits an even narrower main lobe than

at 28 GHz. The antenna's directivity rises to an even higher value because its energy emission focuses on an exact direction that benefits point-to-point communication systems. The narrow beam width enhances antenna performance by reducing signal losses and the likelihood of interference from adjacent channels or signals. The antenna's distinctive feature makes high-frequency applications more precise and efficient due to its capabilities. In both the electric field plane and magnetic field

plane, the total energy or pattern is directed toward the intended propagation direction. Through this process, the antenna radially concentrates its energy transmission, which maximizes power strength toward the path of communication. A reliable communication link becomes possible in dynamic conditions because the antenna demonstrates equally consistent patterns in both planes that do not depend on receiver orientation.

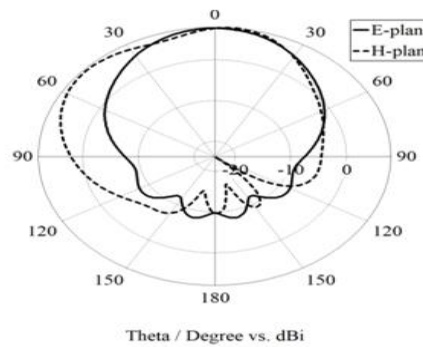


Figure 4: Radiation characteristics operating at 29 GHz

The antenna displays versatile operation and effectiveness at three different frequencies, from 26 GHz to 29 GHz. At 26 GHz frequency operation supports broad pattern generation needed to reach wide coverage areas for mobile applications. Higher transmission frequencies, at 28 and 29 GHz, use focused patterns that boost signal direction while strengthening transmission strength for efficient 5G network communication.

\Evaluation of Surface Current Distribution (SCD of Antenna

The operation of the semi-circular patch antenna depends on the vector surface currents across various frequencies.

Analysis of Surface Current Distribution of Antenna Operating at different frequencies

Figure 5 demonstrates how the current intensity achieves its maximum value at the edges of the patch operating at 26 GHz. The increase in intense radiation is standard for patching antennas because it occurs specifically in the antenna edges. This frequency causes the feed line current to display a sine wave pattern because it is a result of standing wave resonance.

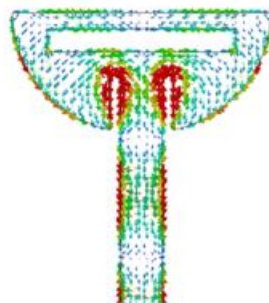


Figure 5: Surface Current Distribution of Single Antenna Element at 26 GHz

The radiation pattern at 28 GHz, depicted in Figure 6, shows a more focused main lobe compared to the pattern at 26 GHz. This indicates an increase in directivity, meaning that more radiated energy is concentrated in a specific direction. A more focused pattern is advantageous for 5G applications that

require targeted communication, as it boosts the signal strength and quality in the desired direction while attenuating interference from other directions. This increased directivity helps in maintaining strong and reliable connections in high-density urban environments.

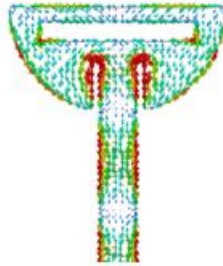


Figure 6: Surface Current Distribution of Single Antenna Element at 28 GHz

At 29 GHz, also depicted in Figure 7, the surface current intensity at the patch's edges is even higher than at 28 GHz, demonstrating that the antenna's radiating efficiency improves with frequency. The strong edge currents suggest that the antenna is

highly effective at radiating energy at this frequency, which aligns with the observed narrow radiation pattern. The sine wave pattern of the current on the feed line remains evident, ensuring stable and effective energy distribution to the patch.

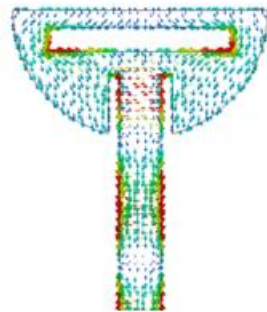


Figure 7: Surface Current Distribution of Single Antenna Element operating at 29 GHz

Design and Simulation of MIMO Antenna operating at 28 GHz

In addition to the single semicircular patch antenna, a MIMO antenna system consisting of two elements has been designed to enhance communication performance for 5G applications. Figures 8 and 9 illustrate the top and bottom perspectives of MIMO antenna. The MIMO configuration employs a Rogers RT/duroid 5880 substrate, acclaimed for its low dielectric constant and minimal loss tangent, which enables superior performance and efficiency at high frequencies.

The T-shaped slot etched from the ground plane functions as an effective method to lower the electromagnetic interference that occurs between two antenna elements. The antenna elements benefit from this T-shaped slot, which reduces the electromagnetic interference between closely spaced elements. When the T-shaped slot is added, it breaks the surface current paths, thus resulting in substantial coupling reduction. The T-shaped slot in the design allows antenna elements to work independently, which enhances MIMO system performance by improving isolation while increasing Channel capacity for 5G communication needs.

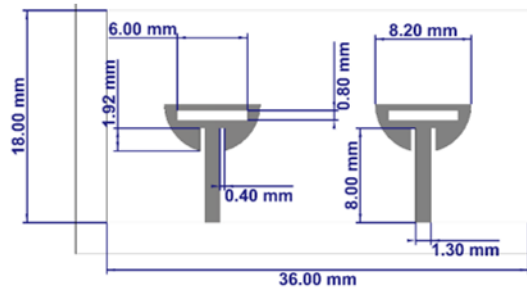


Figure 8: Top view of MIMO Antenna

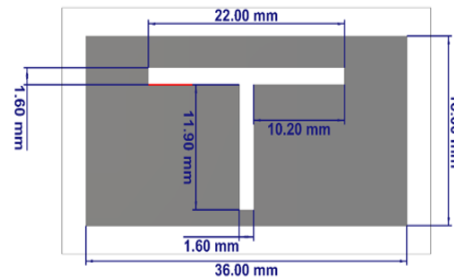


Figure 9: Bottom view of MIMO Antenna

Performance Analysis of MIMO Antenna

The two-element MIMO antenna system performance is evaluated through the S-parameter examination of S11 and S21, as shown in Figure 10. The S11 reflection parameter stays under -10 dB throughout the 28 GHz through 30 GHz frequency band. The antenna demonstrates effective impedance matching with very low signal reflection across its frequency range from 28 to 30 GHz, which enables optimized signal reception and transmission.

The S21 parameter evaluates the degree of mutual coupling between the two antenna components. Subsequent to the inscription of the T-shaped groove in the ground plane, S21 is seen to be below -20 dB over the same frequency spectrum (28 GHz to 30 GHz). The low S21 value indicates superior isolation between the antenna elements, essential for MIMO efficiency since it diminishes interference and enhances signal quality.

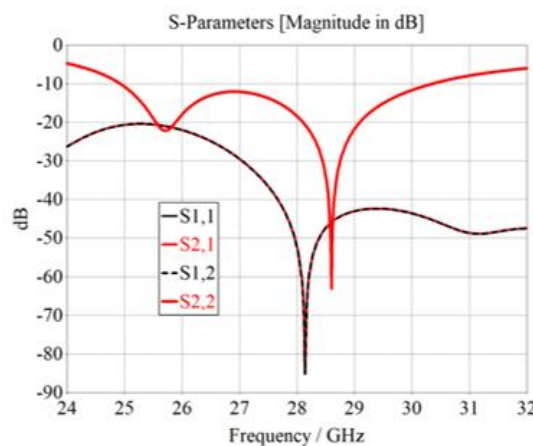


Figure 10: S-Parameters of MIMO Antenna

Figure 11 depicts the diversity gain, which stays close to 10 across the entire frequency range. The diversity

gain (GD) calculation uses the S-parameter information according to the following formula:

$$G_d = 10 \log_{10} \left(\frac{2}{1 - |ECC|^2} \right) \quad (1)$$

ECC denotes the envelope correlation coefficient. The almost 10 dB diversity gain signifies that the

MIMO antenna substantially enhances signal quality and reliability by employing spatial variety to mitigate multipath fading and increase the system efficiency.

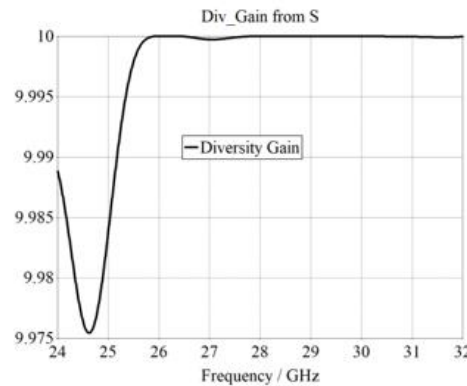


Figure 11: Diversity Gain

The effectiveness of MIMO antennas depends on the evaluation of the ECC, as depicted in Figure 12. In this case, the ECC is nearly equal to 0, which is ideal for MIMO systems. A low ECC value indicates that the antenna elements are effectively uncorrelated,

meaning they can provide independent communication channels. This enhances the capacity and efficiency of the MIMO system, allowing for better exploitation of spatial multiplexing and diversity gains.

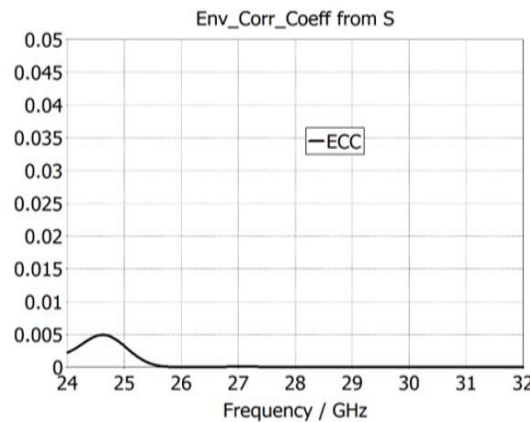


Figure 12: Envelope Correlation Coefficient

Surface Current Distribution of Dual Element MIMO Antenna

The vector surface current distribution of the two-element MIMO antenna shows valuable performance information regarding element interactions and frequency performance. The surface current reveals important characteristics when one antenna element operates while the other matches with a 50-ohm resistance load at 26GHz, 28GHz, and 29GHz. The current surface distribution of proposed design with T-shape slot and without T-shape slot at 26GHz,

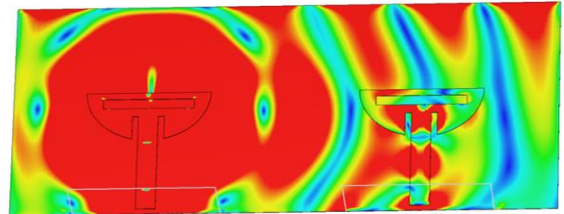
28GHz, and 29GHz are shown in Figure 13, Figure 14, and Figure 15. The port-1 is excited, and port-2 is terminated for better understanding of mutual coupling mechanism. In without decoupling structure most of the current is distributed on excited element and coupled to terminated element, which shows strong mutual coupling between elements. Similarly, in with T-shape decoupling structure, most of the current is distributed on excited elements and remaining current is

neutralized on T-shape slot, which reduce mutual coupling between radiating elements.

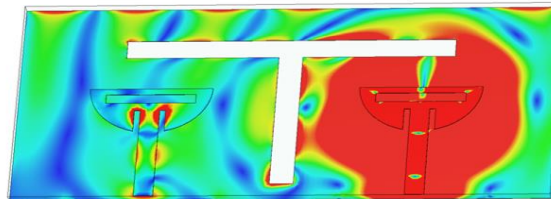
Surface Current Distribution of Dual Element MIMO Antenna at 26 GHz

In Figures 13(a) and 13(b), the surface current reaches maximum intensity on the actual antenna's

edges at the 26 GHz frequency compared to the antenna with the 50-ohm load. The higher edge current level shows that the excited element produces radiation. This frequency generates a sine wave pattern in the feed line current, which represents efficient power transmission through resonance.



(a)



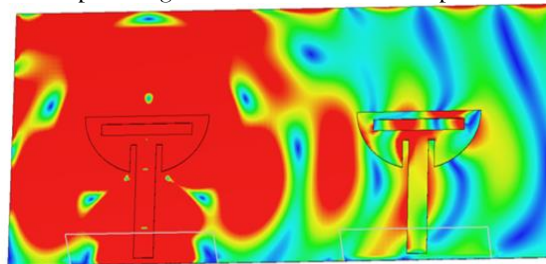
(b)

Figure 13: Surface Current Distribution of MIMO Antenna at 26GHz (a) without stub (b) with T-slot

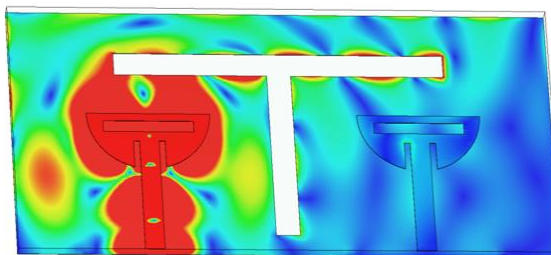
Surface Current Distribution of Dual Element MIMO Antenna operating at 28 GHz

Figures 14(a) and 14(b) illustrates the surface current distribution that appears more intense at the edges of the excited antenna element when operating at 28

GHz. Higher edge current intensity results in better radiation efficiency and directivity characteristics at the elevated frequency. The continuation of the feed line sine wave pattern shows stable performance and effective power transfer to the radiating patch.



(a)



(b)

Figure 14: Surface Current Distribution of MIMO Antenna at 28GHz (a) without stub, (b) with T-slot.

Surface Current Distribution of Dual Element MIMO Antenna operating at 29 GHz

At 29 GHz, also illustrated in Figures 15(a) and 15(b), the current intensity at the edges of the excited antenna element is at its peak, reflecting the antenna's optimal performance at this frequency.

The strong edge currents suggest maximum radiating efficiency, aligning with the focused radiation patterns observed. The sine wave pattern on the feed line continues to be evident, ensuring reliable power delivery to the antenna element.

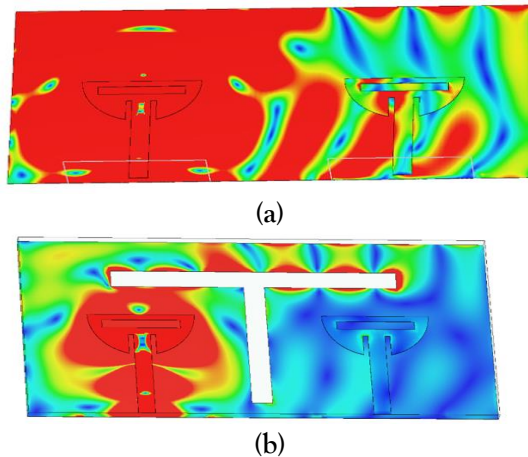


Figure 15: Surface Current Distribution of MIMO Antenna at 29GHz (a) without stub (b) with T-slot

Performance analysis of Single and dual Element MIMO Antennas

Figure 16 illustrates the total efficiency of the single-element antenna and dual-element MIMO antenna designs. Efficiency (η) measures the effectiveness of the antenna in converting input power into radiated power. The calculation may be performed using the below equation:

$$\eta = \frac{P_{rad}}{P_{in}} \tag{3}$$

The efficiency of the single-element antenna and the dual-element MIMO antenna increases across the

frequency band of 25-30 GHz. Notably, the efficiency exceeds 0.85 (or 85%) throughout this range. This high efficiency indicates that the antennas are highly effective at radiating the input power, minimizing losses due to reflections, absorption, and other inefficiencies. The consistent high efficiency within the desired frequency range highlights the suitability of these antenna designs for 5G applications, where high efficiency is critical for maintaining strong, reliable signals.

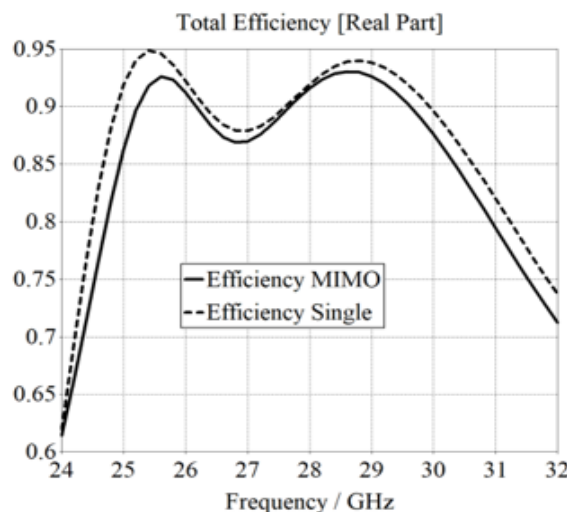


Figure 16: Performance Analysis of Single and Dual MIMO

Radiation Characteristics of MIMO Antenna at different operating frequencies.

Figures 17, 18, and 19 illustrate the radiation characteristics of the MIMO antenna in the electric and magnetic field planes at various frequencies. These patterns demonstrate the antenna's energy radiation in diverse directions across many frequencies.

Radiation Characteristics of Dual Element MIMO Antenna operating at 26 GHz

The radiation characteristics in-terms of both the electric field plane and magnetic field plane operating at 26 GHz exhibits a broad main lobe as shown in Figure 17, indicating that the antenna radiates effectively over a wide angular range. This broad coverage is beneficial for providing consistent signal strength in multiple directions.

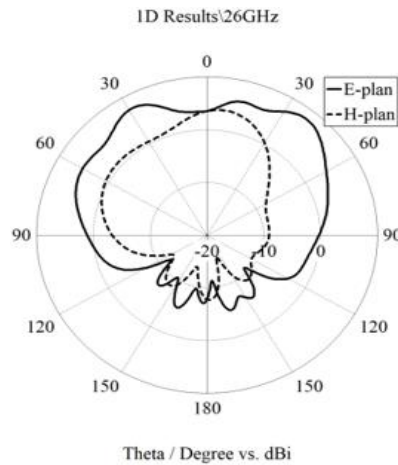


Figure17: Radiation characteristics of MIMO Antenna operating at 26 GHz

Radiation Characteristics of Dual Element MIMO Antenna operating at 28 GHz

The radiation pattern transitions to a focused pattern, as shown in Figure 18, while the main lobe becomes more concentrated in both electric field and magnetic field planes. The antenna directs more

radio energy in particular directions at 28 GHz, which results in superior signal strength and diminished interference from other signal sources. Targeted communication during 5G network operation becomes more efficient because of this directional pattern.

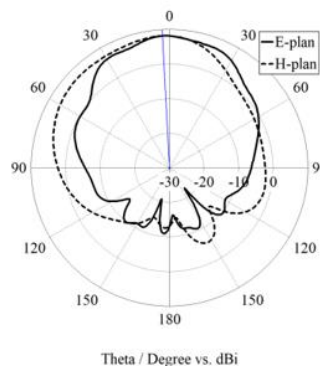


Figure 18: Radiation characteristics operating at 28 GHz

Radiation characteristics of Dual Element MIMO Antenna operating at 29 GHz

At 29 GHz, as depicted in Figure 19, the radiation pattern is even more concentrated, with a very

narrow main lobe in both planes. This high directivity shows that the antenna is highly efficient at directing energy in the desired propagation direction, which is critical for maintaining strong,

focused communication links in high-density environments.

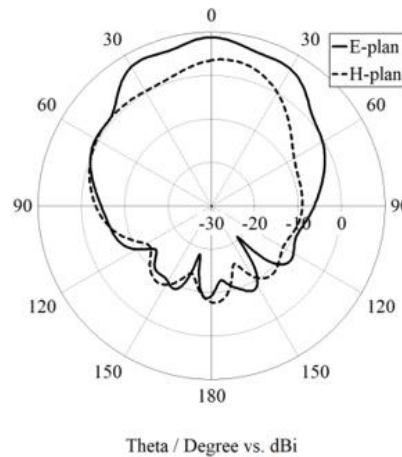


Figure 19: Radiation characteristics operating at 29 GHz

Comparison of the current study with prior work.

This study exhibits substantial advancements compared to prior research on performance and efficiency. It attains the most gain among current investigations, providing improved signal strength and coverage while preserving a compact form factor, in contrast to references [32], [33], and [34]. The suggested approach surpasses others in bandwidth,

rendering it especially appropriate for high-capacity 5G communications. The low Equivalent Current Coupling (ECC) value signifies robust performance, demonstrating minimum correlation between antenna elements, which enhances the system's overall efficacy. Table 1 compares the suggested research with contemporary studies, emphasizing its benefits regarding gain, bandwidth, and ECC.

| Reference | Dimensions (mm ³) | No. of Ports | Frequency (GHz) | Bandwidth (GHz) | Gain (dBi) | ECC (dB) |
|------------|-------------------------------|--------------|-----------------|-----------------|------------|----------|
| 76 | 30 x 30 x 1.575 | 4 | 28 | 4 | 7.1 | 0.005 |
| 77 | 7.2 x 14.4 x 0.254 | 2 | 28 | 4.62 | 7 | 0.01 |
| 78 | 40 x 6 x 0.8 | 2 | 24 | 4.44 | 9.8 | - |
| This Study | 18 x 36 x 0.8 | 2 | 28 | 5.6 | 9.999 | 0.005 |

Table 1: Comparison of the proposed work with the existing literature

CONCLUSION

A 28 GHz MIMO Antenna for 5G Communications is designed based on Rogers RT/duroid 5880 as the dielectric substrate, with dimensions of 18mm×36mm×0.8mm. Hence, better results were obtained with a frequency band of 29.5 GHz up to 30.5 GHz. The bandwidth in terms of the input return loss of the designed is 5.6 GHz. The value of reflection coefficient S11, below -10 dB, is observed in frequencies between 24.9 GHz and 30.5 GHz, with improved radiation patterns, making the antenna very suitable for 5G communications. The future work can be extended to machine learning (ML) and AI-based Algorithms for resource

allocation, dynamic antenna selection and beam alignment regarding 28GHZ MIMO.

REFERENCES

- [1] Salih A A, Zeebaree S R, Abdulraheem A S, et al. Evolution of mobile wireless communication to 5G revolution[J]. Technology Reports of Kansai University, 2020, 62(5): 2139-2151.
- [2] Raj T, Mishra R, Kumar P, et al. Advances in MIMO antenna design for 5G: A comprehensive review[J]. Sensors, 2023, 23(14): 6329.

- [3] Sharma U, Srivastava G, Khandelwal M K, et al. Design Challenges and Solutions of Multiband MIMO Antenna for 5G/6G Wireless Applications: A Comprehensive Review[J]. Progress in Electromagnetics Research B, 2024, 104.
- [4] Alharbi T E A, Shastri A, Alzahrani O A, et al. Evaluation of a wideband monopole antenna with tunable stop notches[C]//Antennas and Propagation Conference 2019 (APC-2019). IET, 2019: 1-4.
- [5] Rani P, Tiwari P, Singh T, et al. A compact ground fed UWB antenna with single band notch characteristics[C]//2021 2nd international conference on smart electronics and communication (ICOSEC). IEEE, 2021: 435-440.
- [6] Heath R W, Gonzalez-Prelcic N, Rangan S, et al. An overview of signal processing techniques for millimeter wave MIMO systems[J]. IEEE journal of selected topics in signal processing, 2016, 10(3): 436-453.
- [7] Ahmed R, Islam M F. Slotted Microstrip Patch Antenna for Multiband Application[J]. International Electrical Engineering Journal, 2014, 5(3): 1293-1299.
- [8] Jilani S F, Rahimian A, Alfadhil Y, et al. Low-profile flexible frequency-reconfigurable millimetre-wave antenna for 5G applications[J]. Flexible and Printed Electronics, 2018, 3(3): 035003.
- [9] Tiwari P, Kaushik M, Shastri A, et al. Two element microstrip-fed slot loaded millimeter wave MIMO antenna[C]//2023 International Conference for Advancement in Technology (ICONAT). IEEE, 2023: 1-5.
- [10] Tiwari P, Kaushik M, Shastri A, et al. Simulated design and analysis of highly isolated 5G millimeter-waves MIMO antenna with wideband characteristic[C]//2023 First International Conference on Microwave, Antenna and Communication (MAC). IEEE, 2023: 1-6.
- [11] Adnan N H M, Rafiqul I M, Alam A H M Z. Massive MIMO for fifth generation (5G): Opportunities and challenges[C]//2016 International Conference on Computer and Communication Engineering (ICCCCE). IEEE, 2016: 47-52.
- [12] Ali W A E, Ibrahim A. A compact double-sided MIMO antenna with an improved isolation for UWB applications[J]. AEU-International Journal of Electronics and Communications, 2017, 82: 7-13.
- [13] Ullah H, Cao Q, Rahman S U, et al. Design and performance evaluation of SWB MIMO antenna with tri-notch functionality and mutual coupling suppression[J]. IEICE Electronics Express, 2023, 20(17): 20230246-20230246.
- [14] Ullah H, Cao Q, Khan I, et al. A Novel Frequency Selective Surface Loaded MIMO Antenna with Low Mutual Coupling and Enhanced Gain[J]. Progress In Electromagnetics Research M, 2023, 118.
- [15] Wei P, Wen G. Design of MIMO/smart antenna arrays using different array modules for handheld device[J]. Prog. Electromagn. Res. C, 2021, 115: 111-126.
- [16] Song Z, Zhao S, Li S, et al. High-Isolation Compact MIMO Antenna with Distributed Metamaterial Loading[J]. Progress in Electromagnetics Research M, 2024, 128.
- [17] Wang X, Dong Y. A Four-Port MIMO Antenna System for 5G Mobile Terminals[C]//2020 IEEE Asia-Pacific Microwave Conference (APMC). IEEE, 2020: 69-71.
- [18] Gu X, Peng X H, Zhang G C. MIMO systems for broadband wireless communications[J]. BT Technology Journal, 2006, 24(2): 90-96.
- [19] Hamdan S, Hamad E K I, Mohamed H A, et al. High-performance MTM inspired two-port MIMO antenna structure for 5G/IoT applications[J]. Journal of Electrical Engineering, 2024, 75(3): 214-223.
- [20] Sharma D, Kumar R, Vishwakarma R K. Multi-standard planar compact 4-port MIMO with enhanced performance for ISM/5G NR/C/WLAN/X band applications[J]. Optik, 2022, 269: 169871.

- [21] Balanis C A. Antenna theory: analysis and design[M]. John Wiley & sons, 2016.
- [22] Milligan T A. Modern antenna design[M]. John Wiley & Sons, 2005.
- [23] Son T, Lee H, Kim S. A Secure Coded MIMO System under Imperfect Channel Estimation[J]. IEEE Transactions on Vehicular Technology, 2024.
- [24] A. Goldsmith, S. A. Jafar, N. Jindal et al. Capacity limits of MIMO channels[J]. IEEE Journal on selected areas in Communications, 2003, 21(5): 684-702.
- [25] Chataut R, Akl R. Massive MIMO systems for 5G and beyond networks—overview, recent trends, challenges, and future research direction[J]. Sensors, 2020, 20(10): 2753.
- [26] Yang H, Qamar F, Kazmi S H A, et al. Interference Mitigation in B5G Network Architecture for MIMO and CDMA: State of the Art, Issues, and Future Research Directions[J]. Information, 2024, 15(12): 771.
- [27] Malkowsky S, Vieira J, Nieman K, et al. Implementation of low-latency signal processing and data shuffling for TDD massive MIMO systems[C]//2016 IEEE International Workshop on Signal Processing Systems (SiPS). IEEE, 2016: 260-265.
- [28] Blaunstein N, Yarkoni N. Capacity and spectral efficiency of MIMO wireless systems in multipath urban environments with fading[C]//2006 First European Conference on Antennas and Propagation. IEEE, 2006: 1-5.
- [29] Patra T, ib Sil S, Maity M. Bit Error Rate Performance Analysis of Different Diversity Techniques for various Channels and also modeling the channel effect[C]//2018 2nd International Conference on Electronics, Materials Engineering & Nano-Technology (IEMENTech). IEEE, 2018: 1-8.
- [30] Bhavana K, Krishna P, Nair A K, et al. Efficient Beamforming Techniques in MU-MIMO[C]//2023 3rd International Conference on Pervasive Computing and Social Networking (ICPCSN). IEEE, 2023: 1521-1527.
- [31] Tehrani F, Teymourian H, Wuerstle B, et al. An integrated wearable microneedle array for the continuous monitoring of multiple biomarkers in interstitial fluid[J]. Nature Biomedical Engineering, 2022, 6(11): 1214-1224.
- [32] Hussain M, Mousa Ali E, Jarchavi S M R, et al. Design and characterization of compact broadband antenna and its MIMO configuration for 28 GHz 5G applications[J]. Electronics, 2022, 11(4): 523.
- [33] Gatram M, Karumuri R. Dual-element MIMO wideband 5G radiator using metamaterials at 28GHz[J]. International Journal of Electronics, 2025: 1-20.
- [34] Sharma M, Gautam A K, Agrawal N, et al. Design of MIMO planar antenna at 24 GHz band for radar, communication and sensors applications[J]. AEU-International Journal of Electronics and Communications, 2021, 136: 153747.

